Alexander Krauß, Hendrik Bayer, Christian Volmer,
Ralf Stephan and Matthias A. Hein:

Low-profile antenna for mobile Ka-band satellite communications

Publikation entstand im Rahmen der Veranstaltung:
32nd ESA Antenna Workshop on Antennas for Space Applications :
5 - 8 October 2010, ESTEC, Noordwijk, The Netherlands, 6 S.

LOW-PROFILE ANTENNA FOR MOBILE KA-BAND SATELLITE COMMUNICATIONS

32ND ESA ANTENNA WORKSHOP
ESA/ESTEC, NOORDWIJK, THE NETHERLANDS
5 – 8 OCTOBER 2010

Alexander Krauß, Hendrik Bayer, Christian Volmer, Ralf Stephan, and Matthias A. Hein

RF & Microwave Research Laboratory, Institute for Information Technology,
Ilmenau University of Technology, P.O. Box 100565, 98684 Ilmenau, Germany
e-mail: alexander.krauss@tu-ilmenau.de, telephone: + 49 3677 69 1578

ABSTRACT

This paper describes the concept of a low-profile user terminal antenna intended for mobile bi-directional Ka-band satellite communications. The concept addresses a hybrid electronic and mechanical tracking method. The antenna consists of several two-dimensional leaky-wave antenna panels. Each panel is excited by a slotted waveguide feed, composed of a linear array of circularly polarised slots. This structure offers a reconfigurable radiation pattern. As a proof-of-principle, a rectangular antenna panel for the downlink at 20 GHz was manufactured and measured. The paper describes the design of the panel in detail and presents the results of numerical simulation and measurement.

1. INTRODUCTION

As a consequence of natural disasters or deliberate attacks, local terrestrial communication infrastructure could be destroyed or de-energised. In such a case, the communication systems of authorities and rescue forces would no longer be operational. Since base transceiver stations and switching equipment depend on public power supply and telecommunication networks, the public infrastructure could also affect parts of the *terrestrial trunked radio* (TETRA, [1]) network. Even if remaining infrastructure was still operational, the remaining terrestrial network infrastructure would be heavily overstrained. The communication of rescue forces through the public network would be extremely limited or even impossible. Under such disastrous circumstances, strategic information and current situation reports are very important for the rescue forces. At least voice communication and the transmission of positioning data and images must be guaranteed, in mobile operation.

If terrestrial emergency communication is unavailable, alternative communication links can be established via satellite. With this approach, vehicles can be connected by nomadic or mobile satellite terminals operating, e.g., at Ka-band frequencies. Thus, a connection of local task forces to a distant coordinating office is feasible without the dependence on public infrastructure or communication networks. The use of Ka-band satellite services is on the rise. The high operation frequencies (downlink: 20 GHz, uplink: 30 GHz) favour the use of a satellite spot-beam architecture, which affords the benefit of smaller terminal apertures and lower power levels compared to existing VSAT solutions.

Our work contributes to the public R&D project *MoSa-Ka* (Mobile Satellite Communications in the Ka-band [2]), which deals with the communication scenarios described above. General project objectives are the development, realisation, and demonstration of a bi-directional satellite transmission at Ka-band frequencies, especially for both mobile and nomadic applications, with a backhauling of local terrestrial networks like TETRA, GSM, WLAN, etc. Obviously, this project would foster applications enabled by the German *Heinrich Hertz* mission which will likeley provide Ka-band facilities [3]. Accordingly, the development of our ground segment hardware also accounts for the envisaged payload of the *Heinrich Hertz* satellite.

In addition to a nomadic terminal that uses a high-gain reflector antenna and supports high-data rate communications [4], the focus of *MoSaKa* is also on another terminal employing a low-profile antenna and enabling truly mobile operation. The low height of this antenna and a compact *outdoor unit* (ODU) are very important for such applications. In contrast to the high-gain reflector antenna, the low-profile antenna is intended for the transmission of low and moderate data rates with high reliability and mobility. A challenging consequence of a high reliability under mobile operation is the fast and easy tracking, which can be enabled by a broadened radiation pattern and the use of sub-apertures. The moderate directivity together with a low structural height restricts the available gain and, for a given link budget, the data rate [2]. Conceivable applications of the low-profile antenna are voice communication, transmission of positioning data, and text message services over point-to-point links via satellite (single hop). Furthermore, a hub-station based architecture (double hop) or broadcast communications are also feasible.

The *MoSaKa* project aims at the demonstration of the immanent aspects of the low-profile antenna in a testbed for system validation and real-time measurements. This testbed consists of an antenna mast with satellite payload, a land-mobile channel simulator for different

propagation conditions, and a motion simulator for vehicular movements [2].

2. LOW-PROFILE ANTENNA CONCEPT

2.1. Antenna

We have selected an antenna concept with a reconfigurable circularly polarised radiation pattern. As depicted in Fig. 1, the concept is realised by differently tilted antenna panels, fixed on a rotary disc. Each antenna panel represents a sub-aperture, connected to a frontend module including up- and down-converters.

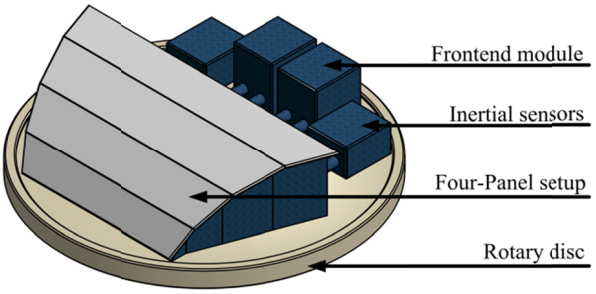

Figure 1. Sketch of the low-profile antenna with tilted antenna panels

Because of the modularity of the antenna assembly, the number and the alignment of the panels are variable. This variability offers an approach to realise different terminal types with specific elevation ranges, for operation in different geographical regions or under different constraints. Furthermore, a manual or automated mechanical pre-adjustment in elevation appears feasible. The use of circular polarisation is highly favourable for a mobile antenna. In contrast to linear polarisation, no acquisition and tracking of the polarisation tilt angle is required, thus lowering the complexity of the antenna system. Our low-profile antenna is expected to apply one circular polarisation for the downlink of a given spot beam, and the orthogonal one for the respective uplink. The maximum height of the antenna shall remain below 15 cm. The principle of using antenna panels can be adopted to both downlink and uplink frequency ranges, thus offering dual-band capability. Our aim is the design of interlaced receive and transmit apertures for a minimal footprint area of the antenna.

2.2. Tracking

The antenna concept addresses a hybrid acquisition and tracking technique that works electronically in the elevation plane and mechanically in the azimuth plane. Tracking in the elevation plane will be accomplished by a radiation pattern that can be reconfigured by activating different antenna panels. As depicted in Fig. 2, there will be at least three differently tilted panels that are able to compensate the variable inclination of a vehicle due to moving. The radiation pattern of each individual panel covers a certain range of elevations, e.g., 20 degrees.

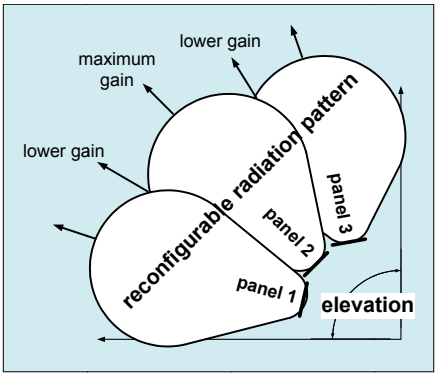

Figure 2. Reconfigurable radiation pattern in the elevation plane

Compared to a switched-beam approach, *maximum ratio combining* (MRC) [5] of the signals received by the sub-apertures and their associated frontend modules enables an improved closed-loop tracking in the elevation plane, though at the expense of an increased number of frontend modules. Fig. 3 illustrates the ODU and the *indoor unit* (IDU) of the mobile satellite terminal.

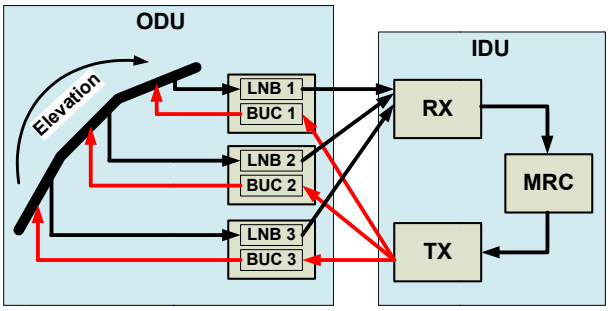

Figure 3. Electronic antenna tracking realised by *maximum ratio combining*

Outdoor unit (ODU), *indoor unit* (IDU), *low-noise block* (LNB), *block up-converter* (BUC), *receiver* (RX), *transmitter* (TX)

The received signals are down-converted simultaneously to an intermediate frequency at L-band and forwarded to the IDU where the signal combining is performed. Especially in the low-gain overlapping range of the elevation patterns of two adjacent panels, MRC delivers a combination gain. Using the MRC-coefficients obtained from the received signals, an appropriate allocation of the transmit apertures can be realised, thus, the antenna beam is also oriented correctly in transmit mode. The *low-noise block* (LNB) and the *block up-converter* (BUC) of one frontend module operate in-phase due to a common local oscillator. According to the number of sub-apertures, several parallel transmit signal lines must be available for the closed-loop tracking. In order to keep complexity and power consumption low, it is important to keep the number of panels minimal.

The tracking of the azimuth will be performed mechanically, supported by the tracking information given by inertial sensors attached on the azimuth positioner. The necessary open-loop tracking information has to be derived from the knowledge of the current location and movement.

3. DESIGN OF A 20 GHZ ANTENNA PANEL

The radiating element selected for the panel is a two-dimensional *leaky-wave antenna.* In general, a leaky-wave antenna is a waveguide-based structure that is able to radiate a significant amount of the available power along its length. A leaky waveguide has a complex wave number, consisting of a phase constant β and a leakage constant α. A leaky-wave antenna radiates in the fast-wave range, thus, the phase constant is smaller than the free-space wave number k_0 [6,7]:

$$\beta < k_0 \tag{1}$$

A two-dimensional leaky-wave antenna can be realised by a *partially reflective surface* (PRS) on a grounded dielectric substrate; the dielectric medium could even be air. A PRS can be considered a metal screen built of a two-dimensional periodic array of specific elements, e.g., patches or slots [8,9]. Due to the partial transparency of such a screen over a ground plane, the power fed into this parallel-plate waveguide structure can leak into space. Inside the dielectric substrate is a primary source like a dipole, a patch antenna, or a radiating slot. Even open-ended waveguides are conceivable, as these are capable of exciting the leaky parallel-plate waveguide structure. The leaky wave propagates outward radially along the periodic surface and leads to an effective antenna aperture determined by the leakage constant α. The value of α can be adjusted through the design of the PRS. If the physical aperture of the antenna is large enough and α sufficiently low, the resulting radiation pattern approaches a pencil beam. For a vertical phase variation corresponding to one half-wavelength inside the parallel-plate waveguide structure, the thickness h of the dielectric substrate is given by [6]:

$$h = \frac{\lambda_0 / 2}{\sqrt{\varepsilon_1 - \sin^2 \theta_0}}, \tag{2}$$

where λ_0 is the free-space wavelength, ε_1 the permittivity of the dielectric substrate, and θ_0 the co-elevation angle of the main-beam direction.

As a first step towards the implementation of a low-profile antenna and a proof-of-principle, a two-dimensional leaky-wave antenna for the Ka-band downlink frequency range at 20 GHz was designed, manufactured, and measured. As depicted in Fig. 4, a 52 mm by 101 mm rectangular PRS composed of a periodic array of metal strips respectively square-patch slots was designed. The width of one metal strip is 3.0 mm and the periodicity is 7.0 mm. Due to the required structural precision, the PRS layer should be realised as a *printed circuit board* (PCB) employing a standard etching process on a *Rogers 4003C* substrate (thickness 0.5 mm). To enable circularly polarised radiation excited by a circularly polarised source, it is important to design the PRS with equal periodicities respectively leakage constants along both Cartesian coordinates.

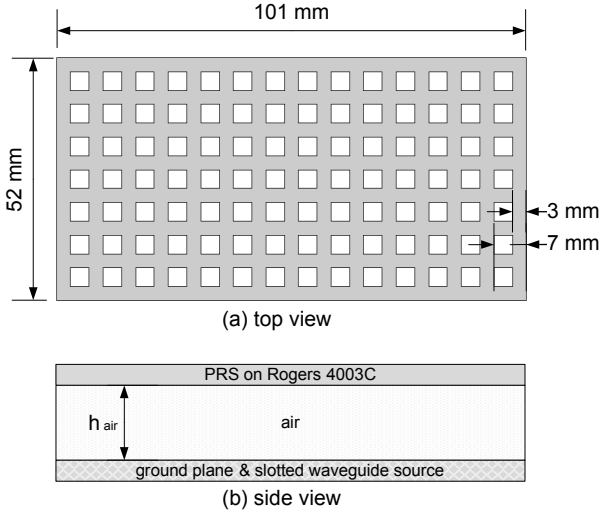

Figure 4. Design of the PRS over a ground plane with integrated slotted waveguide source

The PRS screen on the *Rogers* substrate is located over the ground plane of height h_{air} which is related to the thickness of the dielectric substrate defined by Eq. (2). There is also a weak influence of the permittivity of the Rogers substrate which, due to the small thickness of 0.5 mm, remains marginal. Based on electromagnetic field simulations, the operating frequency was adjusted to 20 GHz, implying a height h_{air} of 6.5 mm.

As depicted in Fig. 4 and further illustrated by Fig. 5, the excitation of the leaky parallel-plate waveguide is realised by a slotted waveguide integrated into the ground plane. The waveguide contains circularly polarised crossed slot radiators [10,11]. A linear five-element array of such slots with a mutual distance of 18.2 mm is arranged on the top of a standard rectangular waveguide (*WR42*). The element separation depends on the guided wavelength in the waveguide and has to ensure the coherent radiation of all five slots.

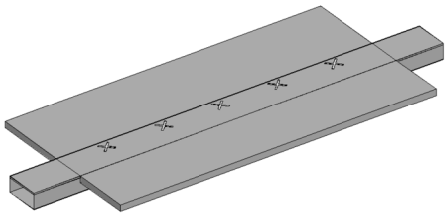

Figure 5. Simulation model of the ground plane-integrated slotted waveguide source composed of a linear array of circularly polarised slots (see lower part of Fig. 4)

To achieve equal field amplitudes at all slots, their lengths vary from 4.6 mm to 5.1 mm depending on their distance from the input port (on the left-hand side in Fig. 5) and their contribution to the overall radiation.
Like the leaky parallel-plate waveguide, the design of the slotted waveguide feeding structure was also based on the principle of leaky-wave radiation, because of its capability to transmit power with low dissipation over a long distance. High efficiency is very important at the high operational frequencies considered here. The two-dimensional leaky-wave antenna panel has the potential of a high total efficiency because of its low number of feeding elements, in contrast to a conventional microstrip patch array.
Due to the rectangular geometry of the panel aperture, the resulting radiation pattern exhibits a broad beam in the elevation plane and a narrower lobe in azimuth, which can partly compensate for the lower gain in elevation.

4. IMPLEMENTATION, MEASUREMENT AND RESULTS

We have manufactured and measured the rectangular antenna panel described above. Fig. 6 shows a photograph of the PRS mounted over a solid body (made of brass) containing the leaky waveguide structure.

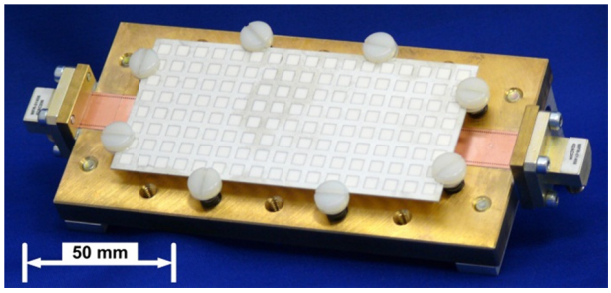

Figure 6. Implementation of a 20 GHz antenna panel with a 52 mm by 101 mm aperture

The PRS was realised as a PCB and attached to the panel module by plastic screws, to adjust the proper height h_{air} = 6.5 mm over the ground plane. Compression springs around these screws helped to optimise h_{air} during measurements. The *WR42* waveguide was milled into a plate made of brass; standard *WR42* flanges were used to connect the antenna panel with the measurement equipment. The two waveguide ports enable the measurement of the transmission coefficient and thus an estimation of the power radiated by the slots and the remaining power transmitted to the output port. The linear slot array was integrated into the top of the *WR42* waveguide. It was also realised on a *Rogers* 4003C substrate, to obtain a high manufacturing accuracy. The substrate material itself is located inside the rectangular waveguide, affecting the dissipation losses in it. This effect was considered in the design process. According to the electromagnetic simulations, the presence of the dielectric substrate led to a slightly reduced distance between the individual slots. The PCB with the slot array on top was soldered into the brass plate, to create a planar ground plane with the integrated slot source.
Fig. 7 compares the simulated and measured magnitude of the forward transmission coefficient S_{21} between the two waveguide ports of the antenna panel over a frequency range from 18 GHz to 22 GHz. The antenna panel was designed to have, at maximum, a magnitude of -10 dB in the range from 19.5 GHz to 20.0 GHz. This value asserts that more than 90% of the input power is radiated, depending on the dissipation losses, and less than 10% coupled to the output port. Furthermore, the input matching should be better than -20 dB over the whole downlink frequency range, which could indeed be verified by measurement.

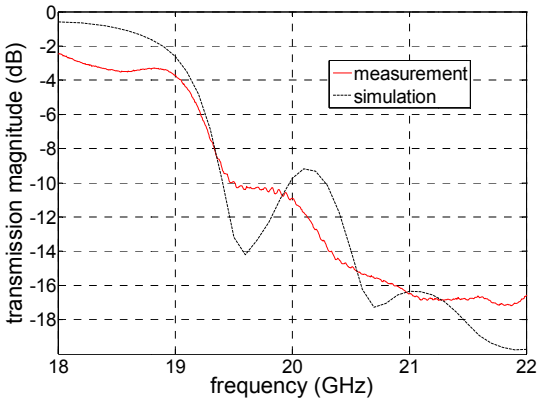

Figure 7. Simulation and measurement of the transmission magnitude in dB between the two waveguide ports of the leaky-wave antenna panel (*WR42* waveguide length: 140 mm)

The simulated and measured results for the radiation patterns were also found in very good agreement. The expected design value of h_{air} = 6.5 mm could be verified. The RHCP (right-handed circular polarisation) directivity pattern of the leaky-wave antenna panel is depicted in Fig. 8 for the elevation plane and in Fig. 9 for the azimuth plane.

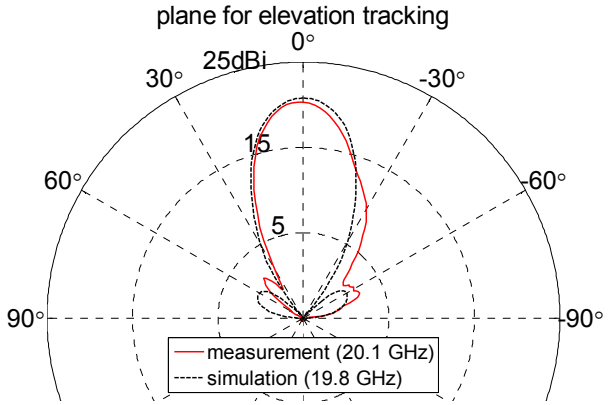

Figure 8. Directivity pattern of the leaky-wave antenna panel across the elevation plane.

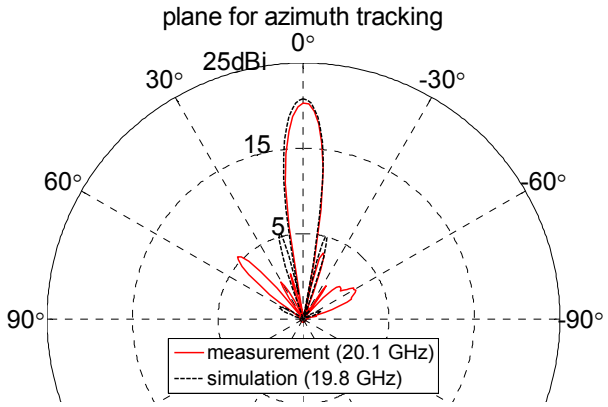

Figure 9. Directivity pattern of the leaky-wave antenna panel across the azimuth plane.

Because of the rectangular geometry of the antenna aperture, in accordance with expectation, the radiation pattern displays a broad lobe with a 3-dB beamwidth of 26 degrees in elevation and a narrower lobe of 8 degrees in azimuth. The main-beam directivity at broadside amounts to 20.8 dBi, simulated at 19.8 GHz, respectively 20.4 dBi, measured at 20.1 GHz. The radiation pattern is slightly deformed in the elevation plane (Fig. 8) due to a small misalignment of the PRS with respect to the slotted waveguide. In the azimuth plane, relevant sidelobes occur at 50 degrees and -60 degrees. Generally, sidelobes in the azimuth plane occur due to the required slot distance of one guided wavelength, needed for coherent excitation [10]. We have identified ways to minimise the sidelobe level in future antenna designs. Furthermore, the realised gain of the antenna panel was measured, in order to evaluate the radiation efficiency and resistive losses, in the frequency range from 18 GHz to 22 GHz.

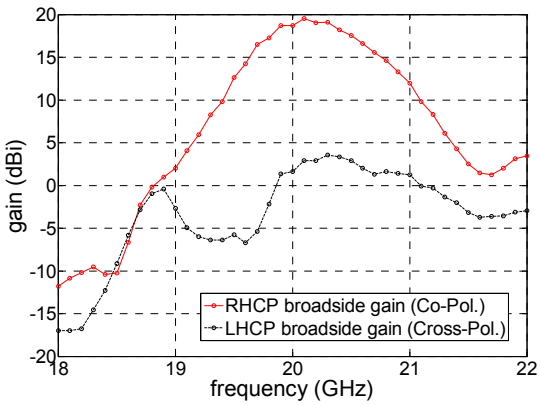

Figure 10. Measured realised gain at broadside for both principle polarisations.

As depicted in Fig. 10, a maximum RHCP gain of 19.6 dBi was obtained at 20.1 GHz. Considering the measured value of the directivity at this frequency (20.4 dBi), the total efficiency of the antenna panel amounts 83 %. The realised gain corresponding to the left-handed circular polarisation was also measured. The plot exhibits a *cross polarisation discrimination* (XPD) exceeding 16 dB around 20 GHz.

5. SUMMARY AND DISCUSSION

A suitable antenna concept for a low-profile mobile satellite terminal antenna was identified and systematically investigated. The concept of this low-profile user terminal antenna can be extended in a modular way, as the number and alignment of the tilted antenna panels can be easily modified. The low-profile antenna assembly offers a reconfigurable radiation pattern that enables maximum ratio combining and an electronic closed-loop tracking in the elevation plane. The leaky-wave antenna panel is excited by a slotted rectangular waveguide structure, composed of a linear array of circularly polarised crossed slots. This feeding structure can be designed equally well for both, downlink and uplink frequencies. The further development will cope with the design challenge of a dual-band structure, given the widely separated up- and downlink frequencies.

As a proof-of-principle, a rectangular leaky-wave antenna panel excited at 20 GHz and applying RHCP was manufactured and measured. The simulation and measurement results were found in good agreement. The main-beam directivity amounted to more than 20 dBi. The total efficiency of the antenna amounted to 83 %. At broadside, a XPD exceeding 16 dB could be verified at the operational frequency.

The possibility to switch between RHCP and LHCP at a given frequency will be investigated in the future. Such a feature would offer an easy mobile handover between adjacent satellite spot beams. As another further development step, the entire low-profile antenna assembly should be tested in a testbed for satellite communica-

tions, to prove its suitability for the envisaged applications.

6. ACKNOWLEDGEMENT

The authors would like to thank M. Huhn and M. Zocher for providing technical assistance. This work has been supported by the German space agency on behalf of the German Federal Ministry of Economics and Technology, project acronym *MoSaKa* (contracts 50YB0913 and 50YB0914).

7. REFERENCES

[1] Stavroulakis, P. (2007). *Terrestrial Trunked Radio – TETRA: A Global Security Tool (Signal and Communication Technology)*, Springer.

[2] Hein, M.A.; Bayer, H.; Krauß, A.; Stephan, R.; Volmer, C.; Heuberger, A.; Eberlein, E.; Keip, C.; Mehnert, M.; Mitschele-Thiel, A.; Drieß, P.; Volkert, T. (2010). *Perspectives for Mobile Satellite Comunictions in Ka-Band (MoSaKa)*, in Proc. of the 4th European Conference on Antennas and Propagation (EuCAP), Barcelona, Spain, pp. 1-5.

[3] DLR Space Agency (2009). *German Satellite Project 'Heinrich Hertz'*, in Countdown 11, issue 3, pp. 3-7.

[4] Bayer, H.; Volmer, C.; Krauß, A.; Stephan, R.; Hein, M.A. (2010). *Tracking Antenna for Mobile Bi-directional Satellite Communication in Ka-Band*, in Proc. IEEE International Conference on Wireless Information Technology and Systems, Honolulu, Hawaii.

[5] Saunders, S.R.; Aragon-Zavala, A. (2007). *Antennas and propagation for wireless communication systems*, John Wiley & Sons, vol. 2, pp. 407-408.

[6] Oliner, A.A.; Jackson, D.R. (2007). *Leaky-wave antennas*, in Antenna Engineering Handbook, 4th ed., McGraw-Hill, ch. 11.

[7] Schühler, M.; Bauer, J.; Krauß, A.; Wansch, R.; Hein, M.A. (2010). *Phase Constant Measurement of Periodically Structured Surfaces – The Leaky-Wave Region*, in IEEE Antennas and Wireless Propagation Letters, vol. 9, pp. 383-386.

[8] Zhao, T.; Jackson, D.R.; Williams, J.T.; Yang, H.Y.; Oliner, A.A. (2005). *2-D periodic leaky-wave antennas – Part I: metal patch design*, in IEEE Trans. on Antennas and Propagation, vol. 53, no. 11, pp. 3505-3514.

[9] Zhao, T.; Jackson, D.R.; Williams, J.T. (2005). *2-D periodic leaky-wave antennas – Part II: slot design*, in IEEE Trans. on Antennas and Propagation, vol. 53, no. 11, pp. 3515-3524.

[10] Simmons, A. J. (1957). *Circularly Polarized Slot Radiators,* in IRE Trans. on Antennas and Propagation, vol. 5, pp. 31-36.

[11] Schäfer, E.; Steinwandt, J.; Bayer, H.; Krauß, A.; Stephan, R.; Hein, M.A. (2010). *Slotted-Waveguide Antennas for Mobile Satellite Communications at 20 GHz*, in Proc. 17th International Student Seminar, Ilmenau, Germany.